

Optimization by simulation of $\text{Cu}_2\text{ZnSn}(\text{S},\text{Se})_4$ thin film solar cell

Abdelkader Benmir

Laboratory of Electrical Engineering (LAGE)

Electrical engineering department, Kasdi Merbah University Ouargla

Ouargla, Algeria

ge.benmira@gmail.com

Abstract— An optimization by simulation of $\text{Cu}_2\text{ZnSn}(\text{S},\text{Se})_4$ thin film solar cell is carried out. It is found that increasing the thickness of the window layer reduces the conversion efficiency of the cell. However, the doping concentration of the buffer layer must have a value at least equal to 10^{16} cm^{-3} . On the other hand, the doping concentration of the absorber layer must be less than or equal to 10^{15} cm^{-3} . In addition, the cell's performance is little variable as long as the defects density of the absorber layer does not exceed 10^{15} cm^{-3} . But as soon as it exceeds this value, a significant decrease is observed. The maximum efficiency that can be achieved with these optimal values is of the order of 13%.

Keywords— Thin film solar cell; $\text{Cu}_2\text{ZnSn}(\text{S},\text{Se})_4$; Optimization; Simulation; CZTSSe

I. INTRODUCTION

An intense research effort has been undertaken to develop thin film solar cells absorbers with abundant, inexpensive and non-toxic elements capable to produce high efficiency devices, economically competitive with conventional energy sources, and support the next-generation in terawatt scale of these solar cells [1]. Copper zinc tin sulfo-selenide $\text{Cu}_2\text{ZnSn}(\text{S},\text{Se})_4$ (CZTSSe) is an excellent absorber and a serious candidate for thin-film solar cells owing to its tunable direct bandgap of 1.0–1.5 eV with a large optical absorption coefficient ($>10^4 \text{ cm}^{-1}$) and p-type conductivity [2]. According to Shockley-Queisser limit, the theoretical conversion efficiency of single-junction CZTSSe solar cells is 32.2 % [3]. These cells are based on a p/n junction which is formed between the p-type absorber and the n-type window. The n-type window consists of a TCO layer and a buffer layer. So far, the highest reported efficiency of SLG/ Mo/CZTSSe/CdS/ZnO:Al thin-film solar cell is 12.6% [4]. In parallel with experimental work, and with the remarkable development of computer tools, the modeling of solar cells [5] has become an indispensable tool for optimizing the design of all types of efficient solar cells. Numerical simulation helps to limit the risk and to avoid the cost of a series of real tests. It will predict the quantitative impact of variations in material properties on device performance and suggest ways to change the deposition process and to improve the performance. The goal of this work is to optimize by simulation the thickness of the ZnO window layer and the doping of the CdS buffer layer as well as the doping and the defects density of the CZTSSe absorber

layer. Following a mathematical model, the simulation is done using the MATLAB programming language.

II. SIMULATION MODEL

A. Structure and optical properties of the cell

The cell structure considered in this study consists of the following materials: ZnO(n) Window / CdS(n) Buffer / CZTSSe(p) Absorber. The solar flux $F(\lambda)$ at $x = 0$ is given by:

$$F(\lambda) = F_0(\lambda).e^{-\alpha_{\text{ZnO}}(\lambda).w_{\text{ZnO}}} \quad (1)$$

Where: $F_0(\lambda)$ is the incident solar flux. $\alpha_{\text{ZnO}}(\lambda)$ and w_{ZnO} are the absorption coefficient and the thickness of ZnO(n) layer respectively. The analytical expressions of the absorption coefficient $\alpha(\lambda)$ for the two materials CdS and CZTSSe can be found in [6] and [7] respectively.

B. Calculation of the photocurrent density, J_{ph}

In all regions, the resolution of the continuity equation combined with Poisson's equation and the current density equation allow us to calculate the current density in each region. Taking into account the phenomenon of generation presented by the rate $G(\lambda, x)$ given by [8]:

$$G(\lambda, x) = \alpha(\lambda)F(\lambda)(1 - R(\lambda)).e^{-\alpha(\lambda)x} \quad (2)$$

Where, $R(\lambda)$ is the fraction of the photons reflected from the front surface. Taking also into account the recombination rates for the electrons in the p-neutral region of CZTSSe presented by $U_n = n - n_0 / \tau_n$ and for the holes in the n-neutral region of CdS presented by $U_p = p - p_0 / \tau_p$ [8]. Where, n is the electron concentration in the p-CZTSSe layer and p is that of the holes in the n-CdS layer. n_0 and p_0 are the equilibrium electron and hole concentrations, respectively. τ_n and τ_p are the lifetimes for electron and hole respectively given by [8]. The total photocurrent density J_{ph} is obtained by integrating the current density $J_{ph}(\lambda)$ on the whole range of the solar spectrum [8]:

$$J_{ph} = \int (J_p(\lambda) + J_n(\lambda) + J_{zce}(\lambda)) d\lambda \quad (3)$$

Where $J_p(\lambda)$, $J_n(\lambda)$ and $J_{zce}(\lambda)$ are the photocurrent density in the neutral zone N (CdS), in the neutral zone P (CZTSSe) and in the space charge region respectively.

C. Solar cell characteristics

The current-voltage (J-V) characteristic of the cell is given by the following equation [8]:

$$J = J_{ph} - J_0 \left(e^{\frac{V+R_s J}{Q R_{sh}}} - 1 \right) - \frac{V + R_s J}{R_{sh}} \quad (4)$$

Where: the saturation current density J_0 is extrapolated according to (5) [9]:

$$J_0 = J_{00} e^{\frac{-E_g}{Q \cdot K \cdot T}} \quad (5)$$

Where: J_{00} is a constant which depend to temperature.

The diode ideality factor Q and J_{00} are extracted from the reference [10].

The numerical solution of (4) for $V = 0$ and $J = 0$ gives respectively the solution as short-circuit current density $J = J_{sc}$ and open circuit voltage $V = V_{oc}$.

From the plot of J-V characteristic, the maximum power, P_m can be calculated. And therefore, we can easily deduce the fill factor and the conversion efficiency which are respectively given by [8]:

$$FF = \frac{P_m}{J_{sc} V_{co}} \quad (6)$$

$$\eta = \frac{P_m}{P_i} \quad (7)$$

Where: $P_i = 100 \text{ mW}\cdot\text{cm}^{-2}$ is the incident power in standard conditions AM1.5G [11].

III. SIMULATION PARAMETERS

The result of our bibliographic research has inspired us the variation ranges of parameters, where:

For the ZnO layer: The thickness, W_{ZnO} varies from 100 to 600 nm [12]. For the CdS(n) layer: The doping, N_d varies from 10^{14} to 10^{20} cm^{-3} [13]. Whereas, for the CZTSSe(p) layer, The doping, N_a varies from 10^{14} to 10^{20} cm^{-3} [14] and the Defect density, N_t varies from 10^{12} to 10^{18} cm^{-3} [15].

The Material and device parameters used in the simulation are shown in Table. I.

TABLE I
DATA VALUES USED IN SIMULATION

Material	CdS	CZTSSe [Ref]
Layer thickness $w(\text{nm})$	50	2500 [16]
Electron Affinity, χ (eV)	4.2	4.1 [16]
Relative permittivity, ϵ_r	10	13.6 [16]
Electron mobility, μ_n ($\text{cm}^2/\text{V}\cdot\text{s}$)	100	100 [16]
Hole mobility, μ_p ($\text{cm}^2/\text{V}\cdot\text{s}$)	25	25 [16]
Donor concentration (cm^{-3}) N_d	1×10^{17}	[17]
Acceptor concentration (cm^{-3}) N_a	-	1×10^{15} [16]
Band gap Energy E_g (eV)	2.42	1.5 [10]
CB ^a Effective density of states, N_C (cm^{-3})	2.2×10^{18}	2.2×10^{18} [16]
VB ^a Effective density of states, N_V (cm^{-3})	1.8×10^{19}	1.8×10^{19} [16]
Hole recombination velocity at CdS front surface, S_p (cm/s)	10^7	[14]

Electron recombination velocity at CZTSSe back surface, S_n (cm/s)	-	10^7 [14]
Defects density, N_t (cm^{-3})	1×10^{17}	1.35×10^{15} [17]
Electron capture cross section, σ_e (cm^2)	10^{-17}	10^{-14} [17]
Hole capture cross section, σ_h (cm^2)	10^{-13}	10^{-14} [17]
General device properties		
Reflectivity, R		0.1 [16]
Series resistance, R_s ($\Omega\text{-cm}^2$)		0.72 [10]
Shunt conductance, G_{sh} ($\Omega^{-1}\text{-cm}^2$)		1610 [10]
Diode ideality factor Q		1.45 [10]
Cell temperature, T (K)		300
^a CB and VB represent the conduction and valence bands, respectively		

IV. RESULTS AND DISCUSSION

A. Thickness effect of ZnO Window layer

Fig. 1 shows the effect of the thickness W_{ZnO} of the ZnO window layer on the cell performance for: $N_d = 10^{17} \text{ cm}^{-3}$, $N_a = 10^{15} \text{ cm}^{-3}$ and $N_t = 1.35 \times 10^{15} \text{ cm}^{-3}$.

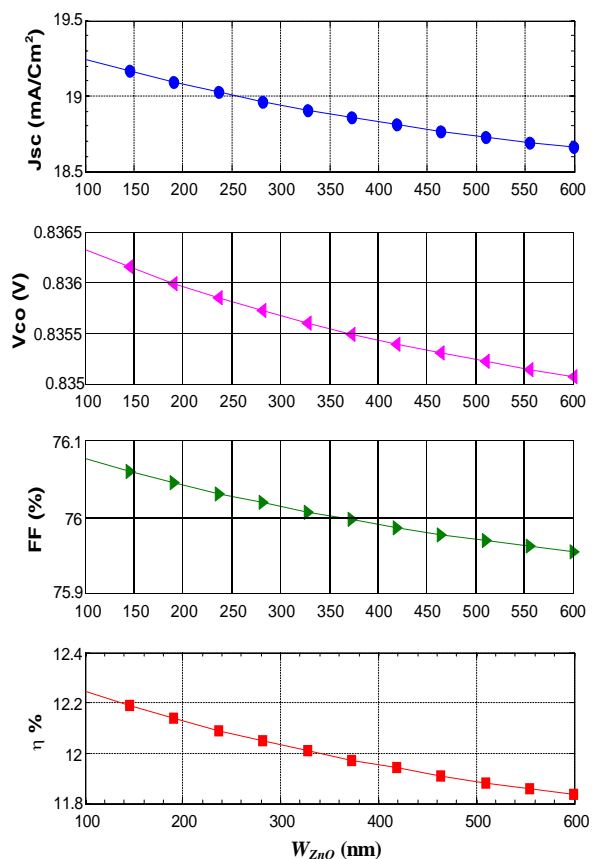


Fig. 1. Cell performance as a function of the window layer thickness

In accordance with (1) and (2), if W_{ZnO} increases, the solar flux $F(\lambda)$ at $x = 0$ and the generation rate $G(\lambda, x)$ decrease. Which decreases the number of electron-hole pairs generated and therefore the decrease in the short-circuit current density J_{sc} . Hence, the decrease in the conversion efficiency η shown in Fig. 1. But, V_{oc} and FF are almost not affected by W_{ZnO} .

B. Doping effect of CdS buffer layer

Fig. 2 shows the effect of the doping N_d of the CdS buffer layer on the cell performance for: $W_{ZnO} = 200$ nm, $N_a = 10^{15}$ cm⁻³ and $N_t = 1.35 \times 10^{15}$ cm⁻³.

We know using the electrical neutrality equation ($N_d \cdot w_1 = N_a \cdot w_2$) that it is the concentration of doping which controls the distribution of the PN junction into zones (Space charge zone $E \neq 0$ where the current is of drift type and the neutral zone $E = 0$ where the current is of diffusion type) on both sides of a PN junction. That is to say, the width of the space charge region on one side of a PN junction increases with increasing of doping concentration on the other side of this junction and vice versa.

So, if N_d increases the space charge zone spreads on the side of CZTSSe absorber layer. Which increases the electric field in this layer and hence, the increase in the collection of charge carriers. Subsequently, a rise in the short circuit current density J_{sc} and the conversion efficiency η .

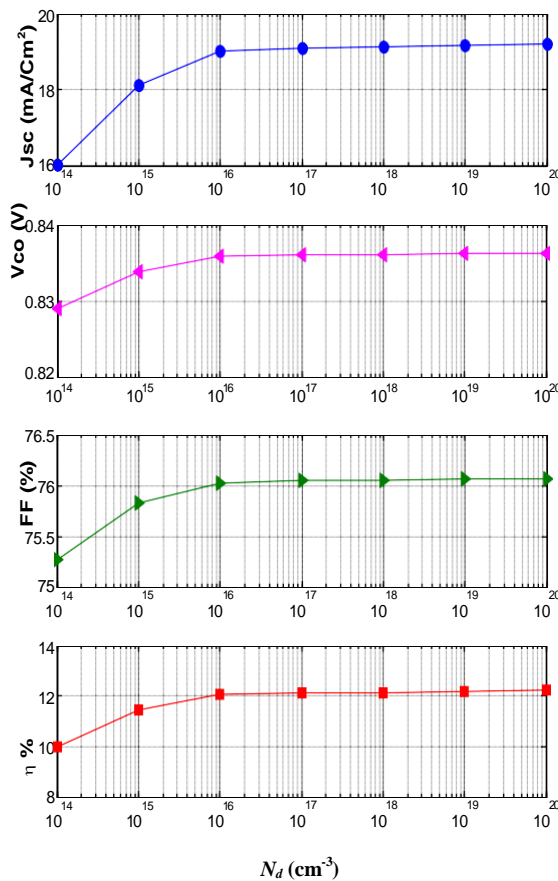


Fig. 2. Cell performance as a function of the buffer layer doping

Therefore, from Fig. 2, the optimal values of the doping concentration of CdS buffer layer are all values where $N_d \geq 10^{16}$ cm⁻³.

C. Doping effect of CZTSSe absorber layer

Fig. 3 shows the effect of the doping N_a of the CZTSSe absorber layer on the cell performance for: $W_{ZnO} = 200$ nm, $N_d = 10^{16}$ cm⁻³ and $N_t = 1.35 \times 10^{15}$ cm⁻³.

As in the previous case, if N_a increases, the space charge zone is reduced on the side of the CZTSSe absorber layer.

This decreases the electric field in this layer and therefore the decrease of the collection of charge carriers. Hence, the decrease in the short circuit current density J_{sc} and the conversion efficiency η .

Therefore, from Fig. 3, the optimal values of the doping concentration of CZTSSe absorber layer are all values where $N_a \leq 10^{15}$ cm⁻³.

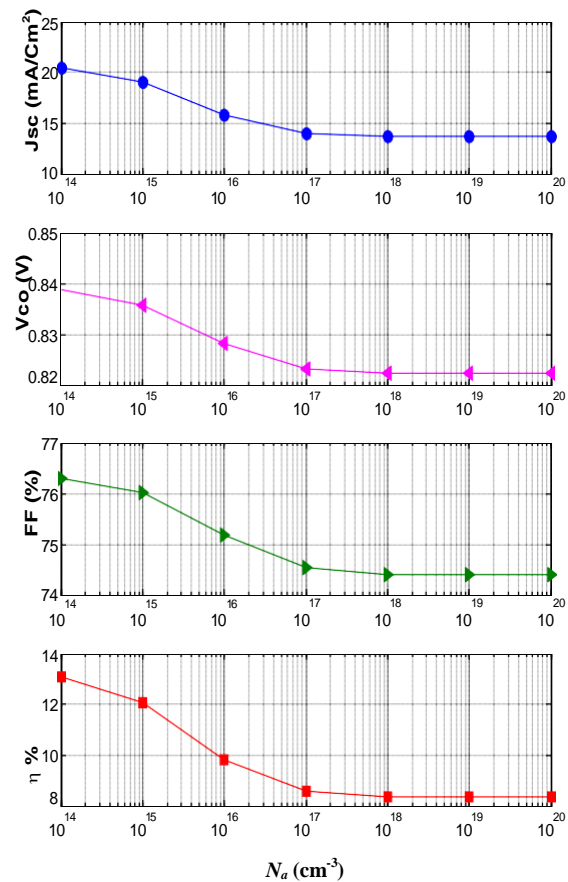


Fig. 3. Cell performance as a function of the absorber layer doping

D. Defects density effect of CZTSSe absorber layer

Fig. 4 shows the effect of the defects density N_t of the CZTSSe absorber layer on the cell performance for: $W_{ZnO} = 200$ nm, $N_d = 10^{16}$ cm⁻³ and $N_a = 10^{15}$ cm⁻³.

We know from equation ($\tau_n = (\sigma_n \cdot v_{th} \cdot N_t)^{-1}$) where $v_{th} \approx 10^7$ cm/s is the thermal velocity that the lifetime τ_n of electrons in the P layer is inversely proportional to the defects density N_t . So, if N_t increases τ_n decreases. This leads, according to equation ($L_n = (D_n^2 \cdot \tau_n)^{1/2}$), to decrease the diffusion length of electrons L_n , and therefore the increase of electron recombination rate. Hence the decrease in the performance of the cell as it is shown in Fig. 4.

It is also clear in Fig. 4 that the performances of solar cell based on CZTSSe absorber are not very variable as long as their defects density does not exceed 10^{15} cm^{-3} . But as soon as it exceeds this value, a significant decrease is observed. Therefore, the optimal values of the defects density of CZTSSe absorber layer are all values where $N_t \leq 10^{15} \text{ cm}^{-3}$. Results similar to these are found by the references [20, 22].

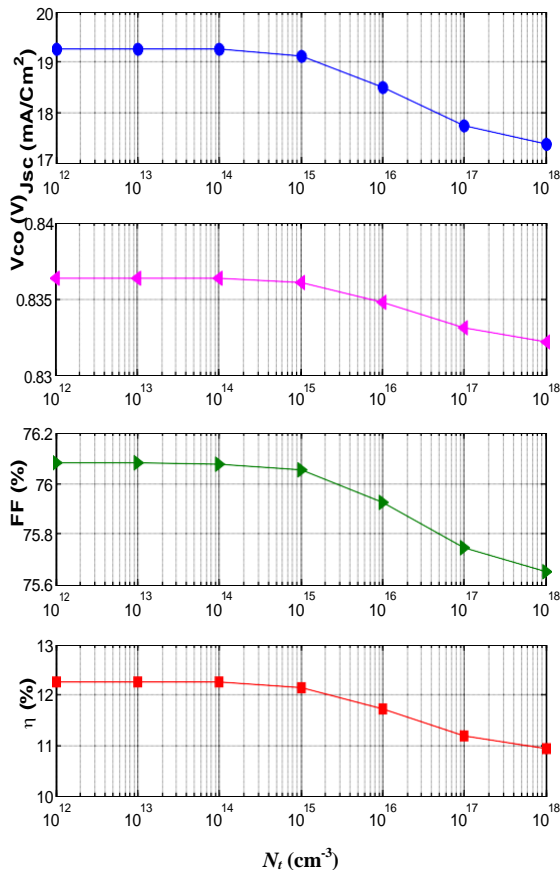


Fig. 4. Cell performance as a function of the absorber layer defect density N_t

V. CONCLUSION

In this work, we made a simulation of a solar cell based on $\text{Cu}_2\text{ZnSn}(\text{SSe})_4$. The calculation program that we have developed allows us to optimize by simulation the thickness of the ZnO window layer and the doping concentration of CdS buffer layer as well as the doping concentration and the defects density of CZTSSe absorber layer.

The obtained results showed that:

The increase of the thickness of ZnO window layer reduces the conversion efficiency η of the cell. However, the doping concentration of CdS buffer layer must have a value at least equal to 10^{16} cm^{-3} . On the other hand, the doping concentration of CZTSSe absorber layer must be less than or equal to 10^{15} cm^{-3} . In addition, the cell's performance is little variable as long as the defects density of CZTSSe absorber layer does not exceed 10^{15} cm^{-3} . But as soon as it exceeds this

value, a significant decrease is observed. The maximum efficiency that can be achieved with these optimal values is of the order of 13%. All these optimization results give helpful indication for feasible fabrication process.

REFERENCES

- [1] D. B. Mitzi et al., —A High-Efficiency Solution-Deposited Thin-Film Photovoltaic Device, *Adv. Mater.*, vol. 20, pp. 3657–3662, 2008.
- [2] D. B. Mitzi, O. Gunawan, T. K. Todorov, K. Wang, S. Guha, —The path towards a high- performance solution-processed kesterite solar cell, *Sol. Energy Mater. Sol. Cells*, vol. 95, pp. 1421-1436, 2011.
- [3] W. Shockley, H. J. Queisser, —Detailed balance limit of efficiency of p-n junction solar cells, *J. Appl. Phys.* vol. 32, pp. 510-519, 1961.
- [4] M. A. Green, Y. Hishikawa, E. D. Dunlop, D. H. Levi, J. Hohl-Ebinger, A. W. Y. Ho-Baillie, —Solar cell efficiency tables (version 51), *Prog Photovolt Res Appl.* vol. 26, pp. 3-12, 2018.
- [5] M. Burgelman, J. Verschraegen, S. Degraeve, P. Nollet, —Modeling thin-film devices, *Prog Photovoltaics Res Appl.* vol. 12, pp. 143-153, 2004.
- [6] M. Jayachandran, M. J. Chockalingam, K. R. Murali, A. S. Lakshmanan, *CuInSe₂ for photovoltaics: a critical assessment*, *Materials Chemistry and Physics*, vol. 34, pp. 1-13, 1993.
- [7] J. J. Scragg, *Copper Zinc Tin Sulfide Thin Films for Photovoltaics Synthesis and Characterisation by Electrochemical Methods*, Ed. Berlin, Germany: Springer-Verlag, 2011.
- [8] S. M. Sze, *Physics of semiconductor Devices*, 2nd ed., Ed. USA: John Wiley & Sons, 1981.
- [9] J. Krustok, R. Josepson, M. Danilson, D. Meissner, *Temperature dependence of $\text{Cu}_2\text{ZnSn}(\text{Se}_x\text{S}_{1-x})_4$ monograin solar cells*, *Solar Energy* 84 379–383 (2010).
- [10] W. Wang et al. , —Device characteristics of CZTSSe thin-film solar cells with 12.6% efficiency, — *Advanced Energy Materials*. Vol. 4, 1301465 (2014) 1-5.
- [11] S. J. Fonash, *Solar Cell Device Physics*, 2nd ed., Ed. USA:Elsevier, 2010.
- [12] S. R. Kodigala, *Thin Film Solar Cells from Earth Abundant Materials, Growth and Characterization of $\text{Cu}_2\text{ZnSn}(\text{SSe})_4$ Thin Films and Their Solar Cells*, Ed. London:Elsevier, 2014.
- [13] A. Morales-Acevedo, N. Hernández-Como, G. Casados-Cruz, —A method for improving their efficiency, — *Materials Science and Engineering B*, vol. 177, pp. 1430–1435, 2012.
- [14] M. Patel, A. Ray, —Enhancement of output performance of $\text{Cu}_2\text{ZnSnS}_4$ thin film solar cells— A numerical simulation approach and comparison to experiments, — *Physica B*, vol. 407, pp. 4391–4397, 2012.
- [15] M. Djinkwi Wanda, S. Ouédraogo, F. Tchoffo, F. Zougmore and J. M. B. Ndjaka, —Numerical Investigations and Analysis of $\text{Cu}_2\text{ZnSnS}_4$ Based Solar Cells by SCAPS-1D, — *International Journal of Photoenergy*, vol. 2016, Article ID 2152018, 9 pages, 2016.
- [16] O. K. Simya, A. Mahaboobbatcha, K. Balachander, —A comparative study on the performance of Kesterite based thin film solar cells using SCAPS simulation program, — *Superlattices and Microstructures*, vol. 82, pp. 248–261, 2015.
- [17] A. Kanevce, I. Repins, S. Wei, “Impact of bulk properties and local secondary phases on the $\text{Cu}_2(\text{Zn,Sn})\text{Se}_4$ solar cells open-circuit voltage,” *Solar Energy Materials & Solar Cells*, vol. 133, pp. 119–125, 2015.